# Granular flow over inclined channels with linear contraction

**D. R. Tunuguntla[1,2]† , T. Weinhart[2], A. R. Thornton[1,2] AND O. Bokhove[1,3]**

[1] Mathematics of Computational Science, Univ. of Twente, The Netherlands
[2] Multi-Scale Mechanics group, MESA+, Univ. of Twente, the Netherlands
[3] School of Mathematics, University of Leeds, UK

(Received 3 December 2024)

We consider dry granular flow down an inclined chute with a localised contraction theoretically and numerically. The flow regimes are predicted through a novel extended one-dimensional hydraulic theory. A discrete particle method validated empirical constitutive law is used to close this one-dimensional asymptotic model. The one-dimensional model is verified by solving the two-dimensional shallow granular equations through discontinuous Galerkin finite element method (DGFEM). For supercritical flows, the one-dimensional asymptotic theory surprisingly holds although the two-dimensional oblique granular jumps largely vary across the converging channel.

**Key words:** Shallow granular flows

## 1. Introduction

Granular flows over inclined channels are a common sight in both natural and industrial environments. Examples range from landslides and debris flows; to the flow of sinter, pellets and coke into a blast furnace for iron-ore melting; down to pouring cereal for breakfast. Besides these applications, it is also of fundamental interest as it allows for precise study of rheological properties of flowing granular material (Pouliquen 1999).

As a stepping stone to predict the dynamics of granular flows over rotating inclined channel, we consider to theoretically analyse flows over inclined channel with localised constriction/contraction, see Fig. 1. For supercritical flows, Vreman *et al.* (2007) observed three different flow regimes: (I) smooth supercritical flow, i.e. with no jumps or shocks or bores (II) flow with a non-steady backward travelling shock or a steady jump upstream of the contraction, and (III) a steady reservoir with a standing jump in the contraction akin to the ones observed by Akers & Bokhove (2008) in their hydraulic chute flow experiments. Motivated by their theoretical means of investigation, we present an extended or novel one-dimensional granular hydraulic model to predict these multiple flow regimes. For closure, we incorporate a discrete particle method validated (Weinhart *et al.* 2012) empirical constitutive law formulated by Pouliquen & Forterre (2002) in contrast to the acceleration integrals used by Vreman *et al.* (2007). Through this one-dimensional asymptotic model, the predicted flow regimes are illustrated on a $F_0 - B_c$ plane where $F_0$ is the channel upstream Froude number and $B_c$ is the critical channel exit width ratio. $B_c$ is defined as the ratio of the channel exit width $W_c$ and the upstream channel

† Email address for correspondence: d.r.tunuguntla@utwente.nl

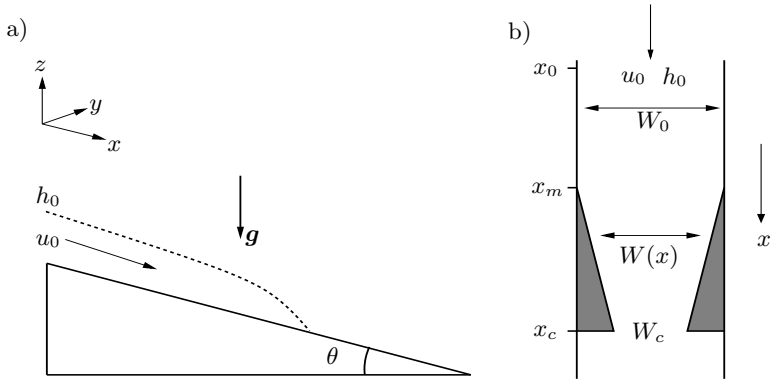


FIGURE 1. a) Illustrates a simple granular flow over an inclined channel. b) Top view of the channel with symmetric sidewall geometry (contraction).

width $W_0$. The one-dimensional asymptotic theory gives a thorough although approximate overview of the flow regimes. Results obtained via this are later verified by solving the two-dimensional granular shallow-layer equations using discontinuous Galerkin finite element method (Tassi *et al.* 2007). Solving them through DGFEM not only helps in verification of the asymptotic theory, due to additional degree of freedom, but most importantly it checks whether the constitutive/friction law holds in higher space dimensions (two dimensions).

$$
\begin{aligned}
h_t + (h\bar{u})_x + (h\bar{v})_y &= 0,\\
\Big(h\bar{u}\Big)_t + \Big(h\alpha\bar{u}^2 + K\frac{h^2}{2}g\cos\theta\Big)_x + \Big(h\bar{u}\bar{v}\Big)_y &= g_n h\Big(\tan\theta - \mu(h,F)\frac{\bar{u}}{|\bar{\boldsymbol{u}}|}\Big) - g_n h\frac{db}{dx},\\
\Big(h\bar{v}\Big)_t + \Big(h\bar{u}\bar{v}\Big)_x + \Big(h\alpha\bar{v}^2 + K\frac{h^2}{2}g_n\Big)_y &= -g_n h\mu(h,F)\frac{\bar{v}}{|\bar{\boldsymbol{u}}|} - g_n h\frac{db}{dy}.
\end{aligned}
\tag{1.1}
$$

## 2. Asymptotic Theory

In rapid free surface shallow flows, the ratio of the velocity and the length scales in the normal to streamwise direction, aspect ratio, is small ($<< 1$). Using long wave approximations, granular shallow-layer equations (1.1) are derived from the general continuum incompressible mass and momentum equations (Savage & Hutter 1989; Wieland *et al.* 1999; Gray *et al.* 2003; Bokhove & Thornton 2012). The above dimensional equations correspond to the conservation of mass and momentum in terms of depth-averaged flow quantities, i.e., flow depth $h = h(x, y, t)$ and velocity $(\bar{u}, \bar{v}) = (\bar{u}(x, y, t), \bar{v}(x, y, t))$ in a channel of width $W = W(x)$. The "$\bar{}$" denotes depth-averaged quantities. $x$ and $y$ denote the down- and cross-slope directions and $t$ is the time. $\mu(h, F)$, $\alpha = \overline{u^2}/\bar{u}^2$ and $K$ is the basal friction coefficient, velocity shape factor and normal stress ratio, respectively. The subscripts $t$, $x$, and $y$ denote the respective partial derivatives and $g_n = g\cos\theta$ is the acceleration due to gravity. $\theta$ is the chute angle chosen such that the average interparticle and particle wall forces are in balance with the downstream force of gravity on granular particles, leading to an uniform flow in the absence of contraction.

With $\alpha = 1$, dropping the "$\bar{}$", using the same aspect ratio argument in cross-slope direction as used for depth-averaging, the flow quantities across the channel are also averaged. On averaging out the y-dependency of the flow quantities, the dimensional

equations (1.1) reduce to *one-dimensional* depth- and width-averaged shallow granular equations

$$\begin{aligned}(hW)_t + (huW)_x &= 0,\\ (hWu)_t + (hWu^2)_x + \frac{1}{2}g_n K W (h^2)_x &= g_n h W\Big(\tan\theta - \mu(h,F)\Big).\end{aligned} \tag{2.1}$$

The averaged flow quantities $h$ and $u$ are independent in $y$ i.e. $h = h(x,t), u = u(x,t)$, with $|\boldsymbol{u}| = |u|$. We consider an uniform channel with a constant upstream width $W_0$ and a localised linear contraction which is monotonically decreasing in width, $W(x) < W_0$, from $x_m$ till it reaches the minimum channel width $W_c$ at $x = x_c$. $x_m$ and $x_c$ denote the $x$ location of the contraction entrance and exit, see Fig. 1b. We always consider the minimum width to be at the end of the channel. For convenience, the shallow-layer model is treated in a non-dimensional form for computational reasons. Thence we introduce the dimensionless variables denoted by primes,

$$\begin{aligned}&t = \frac{W_0}{u_l}t'\,,\; x = W_0 x'\,,\; u = u_l u'\,,\; h = h_l h'\,,\; W = W_0 W'\,,\\ &F_l = \frac{u_l}{\sqrt{g_n h_l}}\,,\; (\tan\theta - \mu(h,F)) = \frac{h_l}{W_0}(\tan\theta - \mu(h,F))'.\end{aligned} \tag{2.2}$$

The variables $W_0$, $u_l$ and $h_l$ are suitable characteristic scales for the length of the mixture motion (usually a reference value of the channel width), flow velocity and depth, respectively. In our model, $W_0$, $u_l$ and $h_l$ are the values defined upstream of the contraction at $x_l = x_0$. The Froude number at $x_l = x_0$ is defined as $F_l = u_l/\sqrt{g_n h_l}$. The average slope of the contraction is given by $\psi = (W_c - W_m)/(x_c - x_m)$. On substituting the scaled variables and dropping the primes, we obtain a non-dimensional depth- and width-averaged shallow-layer model for granular flow.

$$(hW)_t + (huW)_x = 0, \tag{2.3a}$$

$$u_t + uu_x + \frac{K}{F_l^2}h_x = \frac{1}{F_l^2}\Big[\tan\theta - \mu(h,F)\Big]. \tag{2.3b}$$

The scaled 1D shallow-layer equations constitute of a continuity equation (2.3$a$) and a downslope momentum equation (2.3$b$). One could also arrive at these equations via a standard control volume analysis of a column of granular material viewed as a continuum from the base to the free surface, using Reynolds-stress averaging and a leading order closure. Moreover, in order to have a closed system of shallow-layer equations we need a constitutive friction law which is briefly described in the following section.

### 2.1. *Constitutive law/Closure relation*

The basic difference between the shallow-layer fluid model and granular one is the presence of the basal friction coefficient $\mu$, where $\mu$ is the ratio of the shear to normal traction at the base. Few of the previously developed dry granular models incorporated the dry Coulomb-like friction law (Savage & Hutter 1989) implying $\mu$ to be constant, as it equals the tangent of the angle of friction between the material and the base, $\delta$, i.e., $\mu = \tan\delta$. Moreover implying that there is only one inclination $\theta = \delta$ at which steady flow of constant height and flow velocity exists. This is very unnatural. Experimental evidence suggest that the simple Coulomb law is no longer valid on rough beds (Suzuki & Tanaka 1971; Hunger & Morgenstern 1984). Moreover, laboratory investigations concerning flow over rough basal surfaces by Pouliquen (1999), indicated steady flow for a range of inclinations. They formulated an improved empirical friction law characterised by two angles: the angle at which the material comes to rest, $\delta_1$, where friction dominates over gravity

and the angle, $\delta_2$, at which the material accelerates as gravity dominates frictions. It is between these two angles steady flow is possible. They measured the thickness of the granular material, $h_{stop}$, left behind after the flow comes to a halt or when it was brought to rest. The stoppage height as function of angle of inclination is expressed as

$$\frac{h_{stop}(\theta)}{Ad} = \frac{\tan(\delta_2) - \tan(\theta)}{\tan(\theta) - \tan(\delta_1)}\,,\ \delta_1 < \theta < \delta_2 \tag{2.4}$$

where $\delta_1$ is the minimum angle required to flow and $\delta_2$ is the maximum angle at which steady flow is observed, $d$ is the grain diameter and $A$ is a characteristic dimensionless length scale over which friction varies. The relevant expression for the friction law was given by Pouliquen & Forterre (2002) where the Froude number is a linear function of $h/h_{stop}$

$$F = \beta\frac{h}{h_{stop}(\theta)} - \gamma\,,\ \delta_1 < \theta < \delta_2, \tag{2.5}$$

with $\beta$ and $\gamma$ as constants. One can obtain the constitutive law for friction on combining (2.4) and (2.5). Using the steady state flow assumption $\mu = \tan\theta$ to hold(approximately) in the dynamic case as well, one obtains an improved empirical friction law

$$\mu = \mu(h, F) = \tan(\delta_1) + \frac{\tan(\delta_2) - \tan(\delta_1)}{\beta h/(Ad(F+\gamma)) + 1}. \tag{2.6}$$

As $\delta_1 \to \delta_2$, the Coulomb's model is recovered, see Grigorian *et al.* (1967). Furthermore, the above friction law, Eq. (2.6), has been validated by means of discrete particle simulations (Weinhart *et al.* 2012).

### 2.2. *Steady state solutions*

The steady flow regimes are predicted through the closed shallow-layer granular model (2.3$a$) and (2.3$b$) combined with a macro-scale closure relation (2.6). We define a non-dimensional Froude variable as $F = F_l u/\sqrt{h}$. For values $u_0$, $W_0$ and $h_0$ at channel upstream $F_l = F_0$ or $F_l = F_m$ for values $u_m$, $W_0$ and $h_m$ at the contraction entrance $x = x_m$. We retain the parameter $F_l$, $B_c = W_c/W_0$, as well as the scaled $(\tan\theta - \mu(h, F))$ in the momentum equation (2.3$b$).

To begin with, we consider the steady state solutions of (2.3). From (2.3$b$), by introducing non-dimensional Froude variable $F$, we have

$$\frac{d}{dx}\left[\Big(K + \frac{F^2}{2}\Big)h\right] = (\tan\theta - \mu(h, F)). \tag{2.7}$$

Similarly, from (2.3$a$) $huW = Q$, where $Q$ is a constant mass flux. For our scaling we consider $Q = 1$. Substituting this result in $F = F_l u/\sqrt{h}$, we derive

$$h = \left(\frac{QF_l}{WF}\right)^{2/3} \text{ and } \quad \frac{dh}{dx} = -\frac{2}{3}\left[\frac{h}{F}F_x + \frac{h}{W}W_x\right]. \tag{2.8}$$

Combining (2.8) and (2.7), with $K = 1$, results in an ordinary differential (ODE) as below

$$\frac{dF}{dx} = \frac{1}{2}\frac{(F^2+2)F}{(F^2-1)}\frac{d\,[lnW(x)]}{dx} + \frac{3}{2}\frac{[\tan\theta - \mu(F)]}{(QF_l)^{2/3}}\frac{W^{2/3}F^{5/3}}{(F^2-1)}. \tag{2.9}$$

Given a steady flow, for cases where $\mu(h, F) = \tan\theta$ holds (approximately) and $W =$

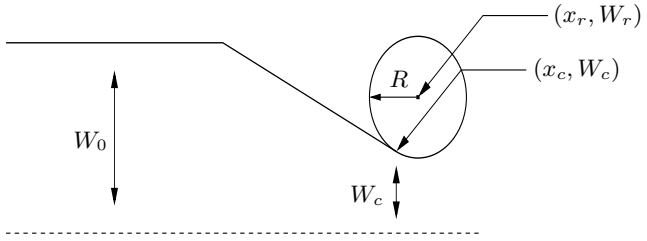


FIGURE 2. $x_c$ in the initial x-location of the contraction exit. $x_r$ is the x-location for the center of the circle used to regularize. For inviscid case, after regularization $x_r$ turns out to be the new x-location for the contraction exit.

$W(x)$, analytical solution to (2.9) is

$$\frac{F_l}{F}\Big(\frac{2+F^2}{2+F_l^2}\Big)^{3/2} = \frac{W}{W_0}. \tag{2.10}$$

Here $W_0$ is the upstream width at at $x_l = x_0$. Similarly, $F_l = F_0$ or $F_l = F_m$ at $x_l = x_0$ or $x_l = x_m$ respectively. The latter being the Froude number at the contraction entrance ($x = x_m$) and the former being the Froude number at the upstream of the channel ($x = x_0$). In the inviscid case, the solution with $F(x_c) = 1$ and for $x \leqslant x_m$, where $F_l = F_0$, is

$$F_0\Big(\frac{3}{2+F_0^2}\Big)^{2/3} = B_c. \tag{2.11}$$

The average solutions obtained are smooth as long as the flow is subcritical with $F_0 < 1$ or supercritical with $F_0 > 1$. The inviscid solution (2.11) divides the $F_0 - B_c$ parameter plane into regions characterising the smooth sub- and supercritical flows, see the thin solid and dashed lines in Fig. 3. The Froude number is constant in the channel upstream whence $F_l = F_0 = F_m$. For the given closed system (2.9), the well known critical channel condition from Houghton & Kasahara (1968), $F = 1$, plays the role of a boundary condition. At this condition the flow at the contraction exit is "sonic" or "critical" such that the flow speed $u$ equals the gravity wave speed $\sqrt{h}/F_l$ which in terms of dimensional quantities mean that the flow speed $u$ equals $\sqrt{g_n h}$. In order to obtain the demarcating curves for granular flows with frictional effects, we integrate ODE (2.9) using the fourth-order Runge-Kutta scheme starting from the contraction exit $x = x_c$ given the critical nozzle condition $F(x_c) = 1$, $B_c$ and width $W = W(x)$. The Froude number $F_l$ and depth $h_l$ at $x = x_l$ is prescribed where $F_l = F_0$ at upstream of the channel or $F_l = F_m$ at the contraction entrance. Rearranging (2.9) and substituting the critical channel condition, $F = 1$, at the contraction exit, $x_c$, indicates

$$\frac{2}{3}\Big(\frac{F^2-1}{F^2}\Big)\frac{dF}{dx} = \Big(\frac{F^2+2}{3F}\Big)\frac{d(ln\, W)}{dx} + \frac{F^{-1/3}W^{2/3}}{(QF_l)^{2/3}}(\tan\theta - \mu(F)), \tag{2.12a}$$

$$\underbrace{0\frac{dF}{dx}}_{LHS} \neq \underbrace{\frac{3}{2}\frac{\psi}{W_c} + \frac{3}{2}\frac{1}{(QF_l)^{2/3}}W_c^{2/3}(\tan\theta - \mu(1))}_{RHS}, \tag{2.12b}$$

a singularity at the contraction exit $x_c$. Note that $\psi = dW/dx$ is the slope at the contraction exit $x_c$. This implies that the ODE doesnt hold at the contraction exit from a mathematical point of view. To resolve the singularity and determine the finite value for $dF/dx$ at the contraction exit we regularise our ODE. Looking at (2.12$b$), the only free parameter that can be varied is the slope of the sidewall, $\psi$. Keeping that in mind, we fit a circle at the exit of the channel as shown in Fig. 2. Choosing a circle seems more

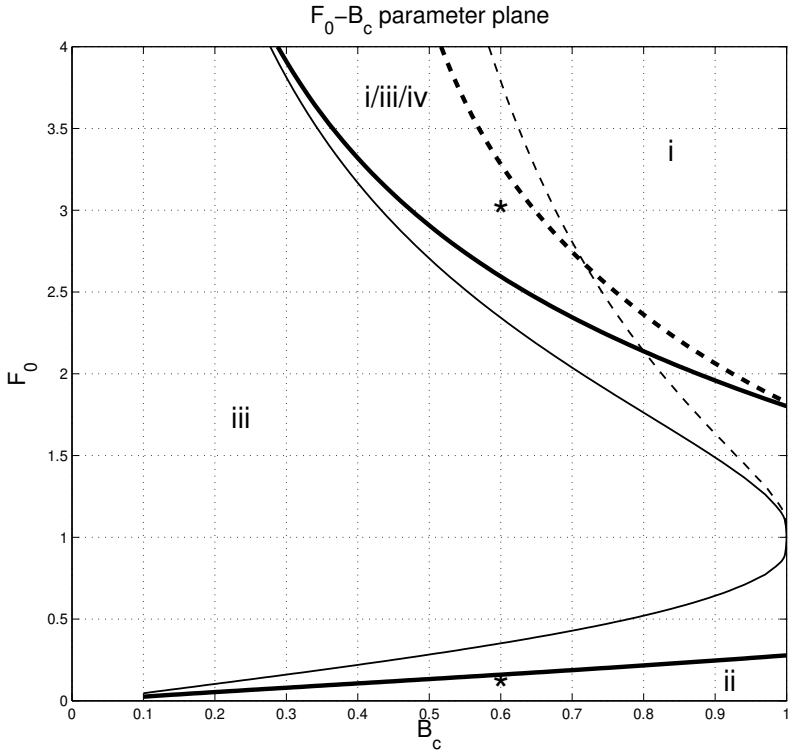


FIGURE 3. The $F_0$, $B_c$ plane is divided into regions of different flow regimes. In region (iii) upstream moving/steady shocks only. In region i/iii/iv, steady shocks in the contraction, upstream moving/steady shocks and oblique waves or averaged smooth flows exists. In region (ii), subcritical smooth flows are distinguished from flows in region iii by the absence of upstream moving shock in the transient stage. In region i, analysis predicts supercritical smooth flows. The solid lines demarcate the existence of the region of super- and subcritical flows for inviscid and frictional flows(thick and thin lines). The dashed lines demarcate the extent of the moving/steady upstream shocks also for viscid and inviscid flows(dashed thick and thin lines).

trivial, as it has infinite number of slopes and can be easily fitted at the contraction exit $x = x_c$. Moreover, as the radius $R \to 0$, one obtains the initial contraction geometry approximately. We find the new contraction exit $x = x_{cnew}$, i.e., $\psi$ for which LHS=RHS. Thence, determine a finite $dF/dx$. With the new contraction exit $x_{cnew}$ at hand, we arrive at a classic limits problem stated as

$$\lim_{x \to x_{new},\, F(x_{new}) \to 1} F' = \frac{dF}{dx} = \frac{0}{0}. \tag{2.13}$$

The limits' problem, (2.13), is solved by using Taylor expansion series. The finite slope $F'$ at the new contraction exit $x = x_{cnew}$ is determined for both inviscid and viscous case. On regularisation, the singularity at the contraction exit, due to the criticial channel condition, is resolved. For given sufficiently large $F_l > 1$ or sufficiently small $F_l < 1$; in order to produce the critical curves between the smooth super- and subcritical flows and flows with jumps, the ODE is integrated from the initial contraction exit either with Froude number $F = \lim_{\varepsilon \to 0} 1 \pm \varepsilon$ or via the regularised approach as described above where we integrate from the channel exit $x = x_{cnew}$ with $F = 1$. Via either approach the

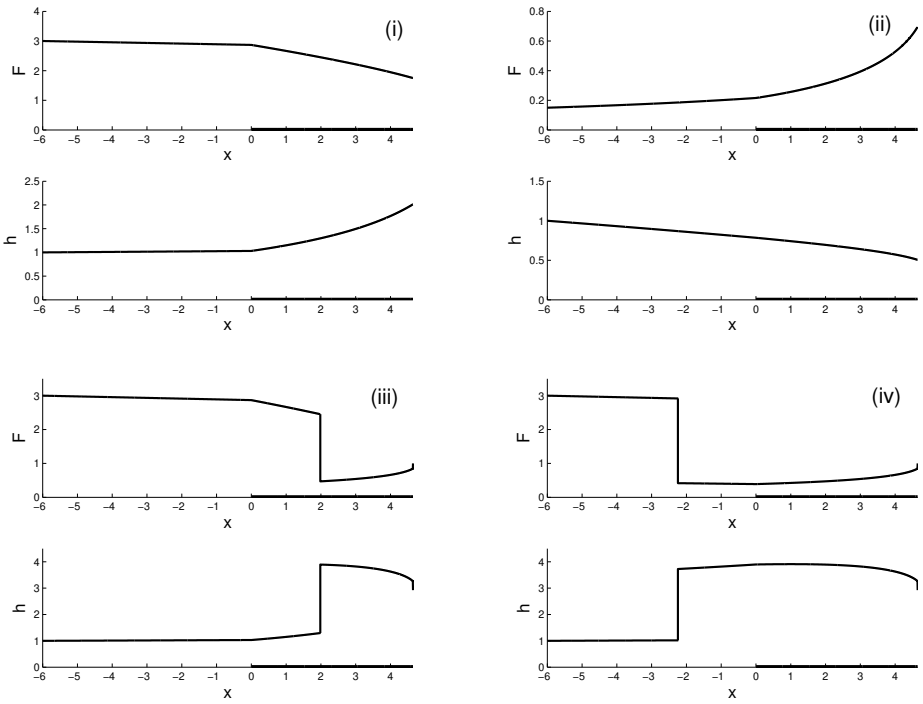


FIGURE 4. Profiles of Froude number F=F(x) and height h=h(x) as a function of downstream coordinate x for the four flow states: (i) Supercritical flow with F >1, (ii) subcritical flow for F< 1, (iii) upstream (steady) shocks, and (iv) reservoir with shock in the contraction. These profiles correspond to the crosses in the $F_0 - B_c$ graph in Fig. 3. The extent of the contraction is indicated by the thick line on the x-axis.

ODE is integrated to a point upstream $x = x_0$ or $x = x_m$ to find a new estimate $F_l^*$. The scaling $F_l$ is unknown beforehand as it is part of the solution. Hence, the solution is found iteratively. As $F_l$ is unknown beforehand, one can consider the initial value for $F_l = F_{0/m}(B_c)$ obtained from the solution for the inviscid case. $F_{0/m}$ is a function of $B_c$. Once the new estimate $F_l^*$ is obtained, we proceed with the newly obtained $F_l^*$ iteratively until convergence is reached. Thereby we obtain the necessary demarcation curves on the $F_0 - B_c$ plane.

### 2.3. *Shock solutions*

The closed system of equations, (2.3), are hyperbolic and thus develop discontinuities in flow fields in finite-time. These discontinuities are nothing but jumps in the depth or velocity of the flow that propagates at a well-defined velocity. For flows with jumps or shocks the critical channel exit condition is $F = 1$. We integrate in the upstream direction, starting from the contraction end, imposing the jump condition by matching the upstream and downstream profiles. For upstream moving shocks instead of matching the upstream conditions with the conditions in the contraction, we relate depth $h_u$ and $u_u$ at the upstream of the shock to $h_1$ and $u_1$ downstream of the shock and also to depth $h_c$ and $u_c$ at the nozzle end. From the mass and momentum balance equations, for a

shock moving at speed $s$ we have the jump conditions as

$$\begin{aligned}(u_u+s)h_u &= (u_1+s)h_1\\ (u_u+s)^2 &= \frac{h_1}{2F_l^2}\Big(1+\frac{h_1}{h_u}\Big).\end{aligned} \tag{2.14}$$

Similarly, we combine the jump conditions with the Bernoulli and continuity equations in the contraction to obtain

$$\begin{aligned}\frac{1}{2}u_1^2+h_1/F_l^2 &= \frac{1}{2}u_c^2+h_c/F_l^2\\ u_1h_1b_1 &= u_ch_cb_c\\ u_c^2 &= h_c/F_l^2\end{aligned} \tag{2.15}$$

When scaled by introducing $F_u = u_uF_l/\sqrt{h_u}$, $S = sF_l/\sqrt{h_u}$, $B_1 = b_c/b_1$ and $H_1 = h_1/h_u$

$$\begin{aligned}\frac{1}{2}[F_u+(1-H_1)S]^2 &= \frac{3}{2}H_1^2\Big[\frac{F_u+(1-H_1)S}{B_1}\Big]-H_1^3\\ (F_u+S)^2 &= \tfrac{1}{2}H_1(1+H_1)\end{aligned} \tag{2.16}$$

As we see when $H_1 = 1$, i.e., when there exists no jump in depth across the shock, the above equation $(2.16)_1$ reduces to purely inviscid case (2.11) for $F_u \leqslant 1$ and $B_1 = B_c$. For $F_u > 0$ and $B_1 = B_c$ it is the thin dashed line in Fig. 3 . The thin solid line for $F_0 < 1$ and the upper thin line is for $F_0 > 1$ divides the $F_0 - B_c$ plane into regions where moving shocks and smooth solutions co-exist. When the viscous term is included i.e. $\tan\theta \neq \mu$, the shocks become steady with time. Hence we consider the shock speed $s = 0$. The Bernoulli equations stated for the inviscid case are no longer valid when we include frictional effects. They are replaced by eq. (2.9) from the shock position to the contraction exit. Similar to the inviscid case, we calculate the arrested shock at the contraction entrance. We integrate (2.9) from the nozzle end to the contraction entrance with the critical channel condition $F = 1$ to the point where the granular jump occurs i.e. at the contraction entrance $x = 0$. If we denote the Froude number just downstream of contraction entrance $F = F_1$ and the upstream as $F = F_m$. Given shock relations with $h_u = h_m$, $u_u = u_m$, $F_u = F_m$, we arrive at $h_1/h_m = [-1+\sqrt{1+8F_m^2}]/2$. With the scaling $Q = 1 = h_1u_1 = h_uu_u$. Hence we obtain

$$F_m = \sqrt{8}F_1/[-1+\sqrt{(1+8F_1^2)}]^{3/2} > 1 \tag{2.17}$$

The ODE (2.9) is further integrated upstream from $F = F_m > 1$ at $x = 0$ to find our next estimate of $F_l^*$ at $x = x_0$. Generally, $F_l^* \neq F_l$ , where $F_l$ is the scaling used in Eqn. (2.9). Thereby, one begins with the inviscid result $F_l = F_0(B_c)$. In the inviscid case one can use (2.10) with $F_l = F_1$ at the entrance of the contraction and $F_m = F_0 > 1$ to find $F_1 = \sqrt{8}F_0/[-1+\sqrt{(1+F_0^2)}]^{3/2}$ from (2.17) to give

$$F_1\Big(\frac{3}{2+F_1^2}\Big) = B_c \tag{2.18}$$

Furthermore, we found that the demarcating curves obtained either by regularisation or non-regularisation to be identical. Nevertheless, the regularisation is necessary to make the numerical analysis mathematically sound.

The flow profiles for super- and sub-critical are illustrated via F, h, and u versus x plots in Fig. 4. These profiles are obtained by integrating from a point upstream of the

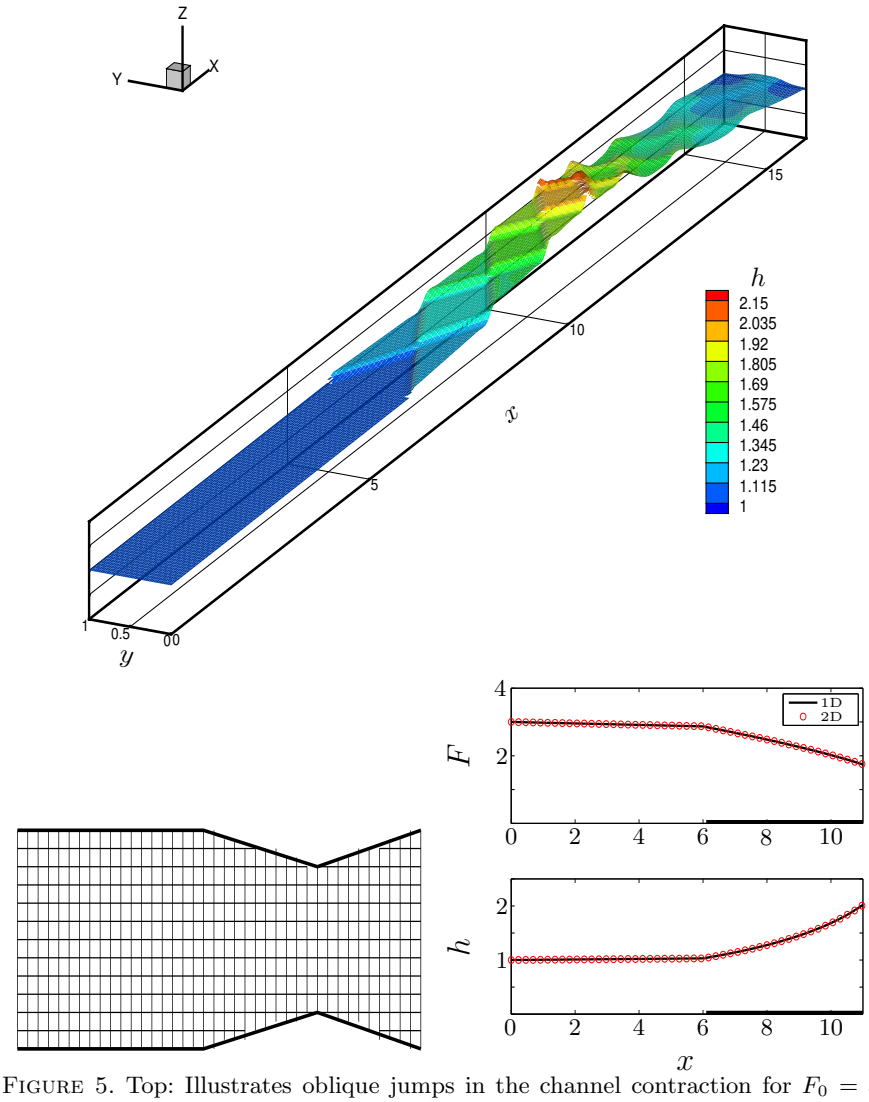


FIGURE 5. Top: Illustrates oblique jumps in the channel contraction for $F_0 = 3$ and channel exit width ratio $B_c = 0.6$. Bottom left: Discretised channel geometry. Bottom right: Cross-slope averaged 2D solutions are compared with the predictions from the theory.

channel into the downstream direction till the contraction exit. For flows with granular jumps, the critical condition at channel exit is $F = 1$. We commence at channel exit into upstream direction and apply the jump condition, where the downstream and upstream profiles match. In the following section, we numerically verify the theoretically predicted flow profile for supercritical flows, $F_0 > 1$.

## 3. Numerical verification

Applying the same initial conditions considered in case (i) of Fig. 4, we solve the two-dimensional system (1.1) through DGFEM (Tassi *et al.* 2007) using an open-source DG solver called hpGEM (hpgem.org). For supercritical flows, flow regime with oblique jumps in the contraction is illustrated in Fig. 5. To compare the steady state solution,

predicted via the theory and obtained via the numerics, we average the 2D flow quantities in the cross-slope direction. On comparing, despite the presence of largely varying oblique jumps across the channel, the solutions agree surprisingly well, see Fig. 5.

## 4. Summary and conclusions

A closed novel one-dimensional granular *hydraulic* theory/model is presented and used to predict multiple steady flow states for flows over inclined channels with localised contractions. For supercritical flows, the predicted solution agrees well when compared to the solution obtained by solving two-dimensional shallow granular equations. Thus, implying that the closure relation holds even in 2D.

For future work, (i) based on the above observations, an ideal scenario would be to validate our model with experiments. As an alternative to them, we will use discrete particle simulations. (ii) Once validated, extend the current analysis to predict flow dynamics over rotating inclined channels.

### 4.1. *Acknowledgements*

The authors would like to thank the Dutch *Technology Foundation STW* for its financial support of project *Polydispersed Granular Flows Over Inclined Channels*. We would also like to thank Sushil Shirsath, Johan Padding, Tim Peeters, Hans Kuipers and Stefan Luding for fruitful discussions.

## REFERENCES

Akers, B. & Bokhove, O. 2008 Hydraulic flow through a channel contraction: Multiple steady states. *Phys. fluids* **20**, 056601.

Bokhove, O. & Thornton, A. R. 2012 *Handbook of Environmental Fluid Dynamics, Fernando H. J. (ed.)*. Boca Raton, FL USA, ISBN:9781-43981-16691.

Gray, J. M. N. T., Tai, Y. C. & Noelle, S. 2003 Shock waves, dead zones and particle-free regions in rapid granular free-surface flows. *J. of Fluid Mech.* **491**, 161–181.

Grigorian, S. S., Eglit, M. E. & Iakimov, I. L. 1967 New statement and solution of the problem of the motion of snow avalanche. *Snow, Avalanches & Glaciers. Tr. Vysokogornogo Geofizich Inst* **12**, 104–113.

Houghton, D. D. & Kasahara, A. 1968 Nonlinear shallow fluid flow over an isolated ridge. *Comm. Pure and Appl. Math.* **21**, 1–23.

Hunger, O & Morgenstern, NR 1984 Experiments on the flow behaviour of granular materials at high velocity in an open channel. *Geotechnique* **34** (3), 405–413.

Pouliquen, Olivier 1999 Scaling laws in granular flows down rough inclined planes. *Physics of Fluids (1994-present)* **11** (3), 542–548.

Pouliquen, O. & Forterre, Y. 2002 Friction law for dense granular flows: application to the motion of a mass down a rough inclined plane. *J. Fluid Mech.* **453**, 133–151.

Savage, S. B. & Hutter, K. 1989 The motion of a finite mass of granular material down a rough incline. *J. Fluid Mech.* **199**, 177–215.

Suzuki, Akira & Tanaka, Tatsuo 1971 Measurement of flow properties of powders along an inclined plane. *Industrial & Engineering Chemistry Fundamentals* **10** (1), 84–91.

Tassi, P. A., Bokhove, O. & Vionnet, C. A. 2007 Space discontinuous Galerkin method for shallow water flows–kinetic and hllc flux, and potential vorticity generation. *Adv. Wat. Res.* **30**, 998–1015.

Vreman, AW, Al-Tarazi, M, Kuipers, JAM, van Sint Annaland, M & Bokhove, O 2007 Supercritical shallow granular flow through a contraction: experiment, theory and simulation. *Journal of Fluid Mechanics* **578**, 233–269.

Weinhart, T., Thornton, A. R., Luding, S. & Bokhove, O. 2012 Closure relations for shallow granular flows from particle simulations. *Granul. Matt.* **14** (4), 531–552.

Wieland, M, Gray, JMNT & Hutter, K 1999 Channelized free-surface flow of cohesionless granular avalanches in a chute with shallow lateral curvature. *Journal of Fluid Mechanics* **392**, 73–100.